



Cite this: *Chem. Commun.*, 2017, 53, 432

Received 25th October 2016,  
Accepted 30th November 2016

DOI: 10.1039/c6cc08595d

www.rsc.org/chemcomm

## An unusual photoconductive property of polyiodide and enhancement by catenating with 3-thiophenemethylamine salt†

Hongtao Yu,<sup>a</sup> Lijia Yan,<sup>a</sup> Yaowu He,<sup>b</sup> Hong Meng\*<sup>ab</sup> and Wei Huang\*<sup>a</sup>

**During our investigation of perovskite solar cell materials, we serendipitously discovered an unusual photoconductive property of polyiodide, which can be enhanced greatly through the interaction of *in situ*-formed polyiodide and 3-thiophenemethylamine salt. This communication examined the photoconductive properties of polyiodide with and without adding different aromatic methylamine compounds. MATPI2 exhibits a high photoconductivity and short response time. The enhanced photoelectric conversion efficiencies are attributed to the strong interaction of polyiodide and the 3-thiophenemethylamine salt.**

Modern research into photovoltaic devices started in the 1950s with the invention of the crystalline silicon solar cell. Since then, photovoltaic concepts have been developed that are based on a variety of solar light absorbing materials, including bulk silicon and semiconductors (GaAs, InP),<sup>1</sup> thin-film polycrystalline or amorphous semiconductors (Si, CdTe, CuInSe<sub>2</sub>, Cu(InGa)Se<sub>2</sub>),<sup>2</sup> semiconductor nanomaterials (nanoparticles, nanowires, quantum dots),<sup>3</sup> organic and metal complex dyes,<sup>4</sup> organic semiconductors (conjugated organic molecules and polymers),<sup>5,6</sup> and organic-inorganic hybrid materials (perovskites).<sup>7</sup>

Over the past few years, solar cells based on metal-halide perovskite absorbers, and in particular organic-inorganic hybrid compounds, have sprung to the forefront of photovoltaic research activity.<sup>8–11</sup> A class of organic-inorganic hybrids is organic-lead trihalide hybrid perovskites. Because of their tunable optical properties, high-absorption coefficients, long-ranged balanced electron and hole transport,<sup>12</sup> low cost and facile deposition techniques,<sup>13–15</sup> organic-lead perovskites have been widely investigated for photovoltaic devices.<sup>16–20</sup> During our investigation of perovskite solar cell materials, we discovered

that the polyiodides of thiophen-3-ylmethanamine can demonstrate an unusual photocurrent effect.

Iodine<sup>21</sup> can catenate through donor-acceptor interactions combined with the influence of counter ions to form polyiodide ions. The Lewis acid acceptor iodine and the Lewis base donors I<sup>−</sup> or I<sub>3</sub><sup>−</sup> can be regarded as the fundamental “building blocks” of polyiodides. To date, several hundreds of polyiodides have been reported in the literature. The reaction of nucleophiles (such as phosphine selenides/sulfides and unsaturated nitrogen) with iodine can also result in the formation of polyiodide species. Iodine has many potential technical applications in a great variety of areas. So far, polyiodide has been widely used in electronics (fuel cells, batteries, solar cells, *etc.*), such as dye-sensitized solar cells, as a reversible redox couple and the organic-lead perovskite as an important component of the inorganic framework for charge transmission. Some reports also indicated that free iodine in the hole transport layer of solar cells can induce valence band trap states to decrease  $V_{oc}$  and increase recombination, leading to the low efficiency of solar cells.<sup>22</sup> Little information has appeared in the literature concerning either the conductivity or the photoconductivity of solid iodine.<sup>23</sup> Photoconductivity studies in iodine single crystals showed that the sustained space-charge-limited photo-current generation at the positive electrode and hole conduction were predominant over electron conduction.<sup>24</sup> However, the photocurrent of iodine single crystals was very low ( $\sim 10^{-10}$  A cm<sup>−2</sup>), which is difficult to meet the practical application. Thus far, the photoconductivity of polyiodide has not been investigated. Herein, polyiodide simply fixed on a rough paper *in situ* can exhibit a certain photoconductive property at a low potential ( $\sim 10^{-5}$  A cm<sup>−2</sup>; 0.1 V), and surprisingly, this property can be greatly enhanced ( $\sim 10^{-4}$  A cm<sup>−2</sup>; 0.1 V) through the interaction with 3-thiophenemethylamine iodine salt by the formation of polyiodides and H-bonding. The strongly coupled iodine hybrid materials afforded a higher performance photoconductive property than did the polyiodide counterpart.

Firstly, we investigate the photoconductive properties of polyiodide as a photoresponsive material. The forming polyiodide *in situ* but iodine can be fixed on a rough paper (Fig. S1, ESI†).

<sup>a</sup> Key Lab for Flexible Electronics & Institute of Advanced Materials, Jiangsu National Synergistic Innovation Center for Advanced Materials (SICAM), Nanjing Tech University, 30 South Puzhu Road, Nanjing, P. R. China.  
E-mail: iamhmeng@njtech.edu.cn, iamwhuang@njtech.edu.cn

<sup>b</sup> School of Advanced Materials, Peking University Shenzhen Graduate School, Peking University, Shenzhen, 518055, China

† Electronic supplementary information (ESI) available. See DOI: 10.1039/c6cc08595d

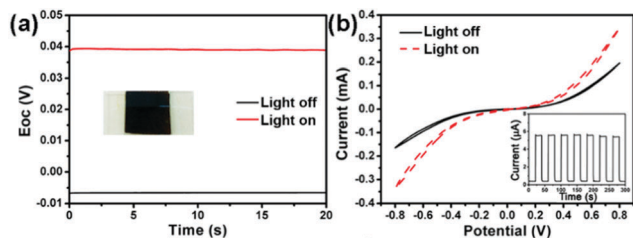


**Fig. 1** (a) Open-circuit potential (the inset shows the photograph of the device (ITO/Polyiodide/ITO)) in the dark and under illumination of a flashlight. (b) Current–voltage characteristics of the polyiodide device in the dark and under  $100 \text{ mW cm}^{-2}$  illumination. The inset shows the time dependence of the photocurrent rise and decay of the device under periodic illumination of a flashlight. The bias is 0.1 V.

The photoelectrochemical performance of polyiodide was tested under a flashlight or  $100 \text{ mW cm}^{-2}$  AM 1.5G simulated solar irradiation. Fig. 1a shows the open-circuit potential ( $V_{oc}$ ) of the simple device of polyiodide/paper, which was sandwiched between ITO (inset of Fig. 1a). Interestingly, an obvious effect was observed under light, increasing  $V_{oc}$  by about 45 mV compared to its value (about 7 mV) in the dark. The low  $V_{oc}$  in the dark can be attributed to the different contents of polyiodide absorbed on the two faces of the rough paper as the substrate. The  $I$ – $V$  curves of the polyiodide device are shown in Fig. 1b. The current increases gradually with potential and the current under light is obviously enhanced compared to the current in the dark. These results reveal that more free-charges are formed under illumination, which indicates the photoconductive characteristic of polyiodide. Upon increasing the polyiodide content on the paper, the  $V_{oc}$  and light current were increased linearly (Fig. S2, ESI<sup>†</sup>), and the maximum light current can reach up to  $30 \mu\text{A cm}^{-2}$  under illumination of a flashlight, which is *ca.* 5 orders of magnitude greater than those of the reported iodine single crystal devices with the same device structure driven by a xenon light.<sup>24</sup> The results of relevant impedance spectroscopy (IS) are shown in Fig. S3 (ESI<sup>†</sup>), which suggest that the increase of electron density resulting from the increase of the electron Fermi level under illumination contributes greatly to the photoconductive behavior of polyiodide.

Surprisingly, the photoconductive behavior of polyiodide can be enhanced through interaction with 3-thiophenemethylamine iodine salt. The fabrication processes of polyiodide/3-thiophenemethylamine/paper devices were the same as those of polyiodide/paper devices, except for the addition of 3-thiophenemethylamine to the original HI solution. As shown in Fig. 2a, the maximum light current was about two times ( $\sim 60 \mu\text{A cm}^{-2}$ ) higher than that of the polyiodide/paper device under the same conditions. By contrast, the Nyquist plots showed only an arc with a linear part resembling a transmission line (TL) behavior in the whole frequency region without the arc for diffusion of holes in Fig. 2b. The equivalent circuit can be simplified to the one shown in the inset of Fig. 2b. These results suggest that the 3-thiophenemethylamine salt can effect the charge transmission of polyiodide, especially for the holes, leading to an enhanced photoconductive property of polyiodide.

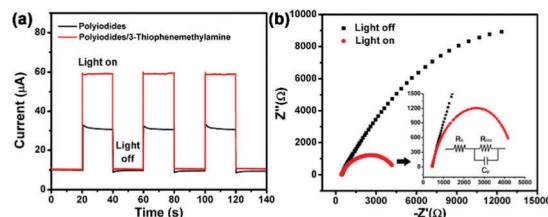
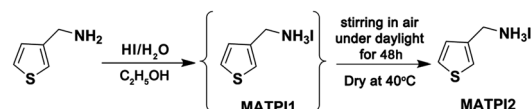


**Fig. 2** (a) Time dependence of the photocurrent rise and decay of the device for polyiodide/paper (black) and polyiodide/3-thiophenemethylamine/paper (red), respectively, under periodic illumination of a flashlight. The bias is 0.1 V. (b) Representative Nyquist plots of the devices for polyiodide/3-thiophenemethylamine/paper in the dark (black) or under a flashlight illumination (red) at short-circuit over the frequency range of 0.1 Hz to 100 kHz. The inset shows the zoom-in of the high frequency region and the equivalent circuit.



**Scheme 1** Synthetic route to MATPI2.

Considering the effect of 3-thiophenemethylamine and to decrease the resistance of the devices, the 3-thiophenemethylamine iodine salt was directly used to fix the polyiodide *in situ* to replace the rough paper. Easy to design, the hybrid (MATPI2) of 3-thiophenemethylamine iodine salt (MATPI1) and polyiodide was synthesized as shown in Scheme 1 (see the Experimental Section). It can be observed that the solution changes gradually from colorless to dark brown under light, which indicates the increasing content of polyiodide. A dark brown crystal (MATPI2) can be obtained after drying it in air. For comparison, colorless 3-thiophenemethylamine iodine salt (MATPI1) was synthesized according to the literature (see the Experimental Section).<sup>16</sup> The appearance of MATPI2 and MATPI1 is shown in Fig. 3. <sup>1</sup>H NMR and <sup>13</sup>C NMR spectra of MATPI1 and MATPI2 were collected on a mercury 300 MHz using CH<sub>3</sub>DO and were referenced to the solvent residual peak (MeOD: <sup>1</sup>H: = 4.87 ppm; <sup>13</sup>C: = 49.00 ppm) (Fig. S4, ESI<sup>†</sup>). The similarity of their spectra suggests that MATPI2 is a mixture of polyiodide and MATPI1, in which the polyiodide can be removed through rinsing with diethyl ether to obtain colorless MATPI1. However, compared to the MATPI1, the proton chemical shift of MATPI2 moves to the lower field, which indicates the formation of a H-bond.<sup>25,26</sup> This result suggests that the active H atom of 3-thiophenemethylamine can make a short contact with the terminal iodine atom of polyiodide.<sup>27</sup> It can be concluded that the polyiodide ion interacts with MATPI1 salt through the ionic interaction with NH<sub>3</sub><sup>+</sup> and H-bonding.

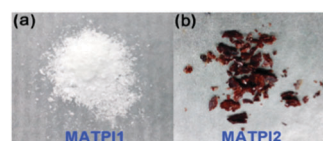


**Fig. 3** Appearance of MATPI1 (a) and MATPI2 (b).

To further confirm the structure of MATPI2, a powder XRD experiment was conducted; the results are given in Fig. S5 (ESI<sup>†</sup>). The peaks corresponding to different crystal planes of MATPI2 are consistent with MATPI1. However, the relative intensities of XRD diffractions for some peaks are decreased greatly, which is probably due to the existence of polyiodide ions, leading to structural disorder.

The devices of MATPI2 were prepared in the same way described above without paper (Fig. S6, ESI<sup>†</sup>). Expectedly, the measured light current density increases significantly by nearly 10 times of magnitude (up to nearly  $200 \mu\text{A cm}^{-2}$ ) as compared to the dark current density of the present device at a bias of 0.1 V and by 3.2 times compared with the light current of polyiodide/3-thiophenemethylamine/paper devices ( $\sim 60 \mu\text{A cm}^{-2}$  at 0.1 V) under the same conditions (Fig. 4a). The present device also shows good reproducibility and stability. Notably, both the rise time and decay time of the present device are shorter than 40 ms at 0.1 V (Fig. 4b). The fast rise and decay could be attributed to the solid-state process in which excitons are generated instantaneously by light and extracted by the electrode.<sup>28</sup> Compared with the devices of polyiodides (Fig. S7, ESI<sup>†</sup>), the MATPI2 obviously exhibited a shorter decay time, indicating a higher extraction efficiency of the separated carriers. Fig. 4c shows the  $I$ - $V$  curves of the MATPI2 devices in the dark and under  $100 \text{ mW cm}^{-2}$  AM 1.5 illumination, which indicate that the current under light is increased obviously and the photocurrent of the device is highly dependent on the bias voltage. The photoenhanced current increases especially upon application of a bias; the current density increases due to the enhanced separation efficiency of geminate charge pairs and the improved extraction efficiency of the separated carriers from the electrodes at higher electric fields.<sup>29</sup> Similarly, as the 3-thiophenemethylamine

was replaced by 2-thiophenemethylamine and benzylamine, the same phenomenon can be observed (Fig. S8, ESI<sup>†</sup>). However, the brown color of the corresponding products becomes shallow (Fig. S8a-c, ESI<sup>†</sup>), leading to a weak ability of the photoelectronic response as well as the current dose under the dark conditions (Fig. S8d-f, ESI<sup>†</sup>). The color of the products is a direct function of the amount of polyiodide present. Compared with 2-thiophenemethylamine and benzylamine, more polyiodide can be fixed by 3-thiophenemethylamine iodine salts, probably due to the extra hydrogen bonding interaction owing to the inherent features of the neighboring effect. Moreover, as the alkyl molecules with the amino group (methylamine or *n*-butylamine) were used, the obtained product was evaporated completely after drying treatment, indicating the weak interaction between alkyl molecules and polyiodide. From these results, we can conclude that the 3-thiophenemethylamine iodine salt not only can fix the polyiodide effectively, but can also enhance the photoconductive property of polyiodide *in situ*. Fig. 4d shows the Nyquist plots of the MATPI2 devices. A similar characteristic to the polyiodide/3-thiophenemethylamine/paper devices, that is, an arc with a linear part resembling a transmission line (TL) behavior at high frequency, can be observed in the dark, which contributed to the transport and recombination process of electrons. Nevertheless, the corresponding contact resistance ( $R_s$ ) was decreased greatly and a symmetrical and intact small semicircle without the TL characteristic was observed under illumination; to fit this part, a simple  $R$ - $C$  circuit is employed (see the inset of Fig. 4d), suggesting a more obvious decrease of charge transfer resistance due to the increased electrical conductivity of the devices as a consequence of the higher electron density under illumination.

To obtain a deeper insight into the role of 3-thiophenemethylamine salt in the performance of polyiodide devices, the UV-Vis absorption spectra of MATPI1, MATPI2 ethanol solutions and MATPI2 thin films are shown in Fig. S9a (ESI<sup>†</sup>). As expected, the absorption curves of the MATPI2 ethanol solutions are consistent with the polyiodide ethanol solution. Moreover, the absorption bands of the MATPI2 solid films extend to larger wavelengths, which results from the formation of more polyiodide ions with the increase of iodine content, and polyiodide network structures start to emerge resulting from the bond between iodine ( $\text{I} \cdots \text{I}$ ).<sup>30</sup> However, when MATPI2 is left under dynamic vacuum or simply in air, it releases the iodine along with shallowing of the brown color and the loss of the photoconductive effect gradually. Raman scattering is strongly sensitive to the electronic structure and proves to be an essential tool to characterize the nature of polyiodide systems.<sup>31-33</sup> The Raman spectra of MATPI2 are shown in Fig. S9b (ESI<sup>†</sup>). The peaks at  $218$ ,  $156$ ,  $110$  and  $67 \text{ cm}^{-1}$  can be observed, which correspond to the fundamental polyiodide building blocks  $\text{I}_2$  and  $\text{I}_3^-$ , indicating the formation of polyiodide. These results can be explained as follows: firstly, the symmetrical ion  $\text{I}_3^-$  normally exhibits one Raman active band, the  $\nu_1$  symmetric stretch at around  $110 \text{ cm}^{-1}$ .<sup>31</sup> However, when the ion is made asymmetric through distortion or interactions with other species (herein  $-\text{H}$ ,  $-\text{NH}_2$  and  $\text{I}_2$ ), the  $\nu_2$  deformation vibration

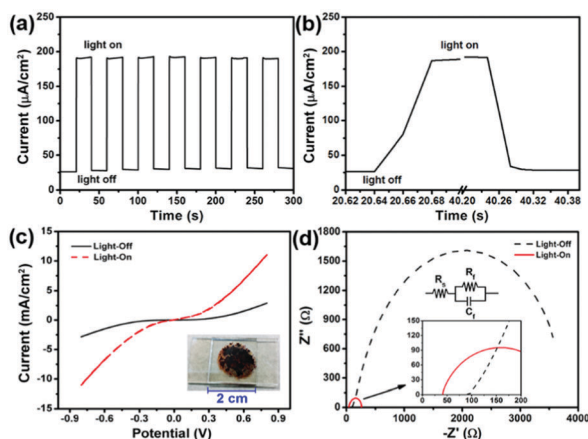


Fig. 4 (a) Time dependence of the photocurrent rise and decay of the device assembled from the MATPI2 under periodic illumination of a flashlight. The bias is 0.1 V. (b) Zoom-in of a part of the photoresponse curve. (c) Current-voltage characteristics of the MATPI2 device in the dark and under  $100 \text{ mW cm}^{-2}$  illumination. The inset shows the photograph of the device (ITO/MATPI2/ITO). (d) Representative Nyquist plots at short-circuit of a simple device in the dark (black and dashed-line) and under illumination (red and solid-line). The inset shows zoom-in of the high-frequency region and the equivalent circuit.

and  $\nu_3$  antisymmetric stretch at approximately 70 and 130–140  $\text{cm}^{-1}$ , respectively, also become Raman active.<sup>32</sup> Secondly, free I-I exhibits a single Raman band at 180  $\text{cm}^{-1}$  in the solid state, which moves to a lower wavenumber upon co-ordination to a donor atom (herein  $-\text{H}$ ,  $-\text{NH}_2$  and  $\text{I}_3^-$ ), indicating a reduction of I-I bond order.<sup>33</sup> Taking the above information into consideration, MATPI2 can be seen as composed of MATPI1 and iodine ( $-\text{NH}_3\text{I} \cdots \text{I}-\text{I}$ ;  $-\text{H} \cdots \text{I}-\text{I}$ ), and the polyiodide network is formed through the bonding interaction of iodine which is crucial for the photoconductive effect of MATPI2 (Fig. S9c, ESI†).

Based on these results, we extrapolated two explanations for the photoconductive performance of polyiodide: on one hand, the polarized iodine absorbs light and forms an exciton that ionizes in an electric field. Electrons can transfer through the network of polyiodide. Some reports have indicated the conductivity of polyiodines.<sup>34</sup> Iodine could be polarized by the adjacent iodine, and this polarization can be enhanced by the interaction of 3-thiophenemethylamine salt, leading to formation of more excitons under illumination. On the other hand, photogenerated excitons from the polarized iodine are separated into electrons and holes by the interaction between the excitons and the hole trap centers on the surface of the 3-thiophenemethylamine salt. More specific work is under way.

To summarize, we revealed the photoconductive properties of polyiodide through a simple device. Unusually, the photocurrent of polyiodide is about  $10^5$  times greater than that of iodine single crystals. Moreover, this property can be greatly enhanced through interaction with 3-thiophenemethylamine iodine salt. The high photoconductivity, the short response time both on rise and decay and the stable photocurrent undoubtedly demonstrate the potential of the strongly coupled polyiodide/organic hybrid as a novel photoelectronic system for OPV applications. This finding opens up a brand new approach to photoelectric materials for energy conversion.

This work was supported by the NSFC (51373075, 61136003), the National Research Foundation (20133221110005), the National Basic Research Program of China (973 Program, No. 2015CB856505; 2015CB932200), the NSFJS (BM2012010), the Shenzhen Peacock Program (KQTD2014062714543296), the NSFCD (2014A030313800), and the Guangdong Talents Project. The authors gratefully acknowledge helpful discussions from Prof. F. Wudl in the Department of Chemistry & Biochemistry, University of California, Santa Barbara.

## Notes and references

- 1 L. Tian and M. Dagenais, *Prog. Photovoltaics*, 2015, **23**, 997.
- 2 C. Reese and Z. Bao, *Mater. Today*, 2007, **10**, 20.

- 3 G. Konstantatos, M. Badioli, L. Gaudreau, J. Osmond, M. Bernechea, F. P. G. de Arquer, F. Gatti and F. H. Koppens, *Nat. Nanotechnol.*, 2012, **7**, 363.
- 4 B. O'regan and M. Grätzel, *Nature*, 1991, **353**, 737.
- 5 R. H. Friend, R. W. Gymer, A. B. Holmes, J. H. Burroughes, R. N. Marks, C. Taliani, D. D. C. Bradley, D. A. Dos Santos, J. L. Bredas, M. Logdlund and W. R. Salaneck, *Nature*, 1999, **397**, 121.
- 6 K. M. Coakley and M. D. McGehee, *Chem. Mater.*, 2004, **16**, 4533.
- 7 A. Kojima, K. Teshima, Y. Shirai and T. Miyasaka, *J. Am. Chem. Soc.*, 2009, **131**, 6050.
- 8 H. J. Snaith, *J. Phys. Chem. Lett.*, 2013, **4**, 3623.
- 9 N.-G. Park, *J. Phys. Chem. Lett.*, 2013, **4**, 2423.
- 10 M. A. Green, A. Ho-Baillie and H. J. Snaith, *Nat. Photonics*, 2014, **8**, 506.
- 11 M. Grätzel, *Nat. Mater.*, 2014, **13**, 838.
- 12 G. Xing, N. Mathews, S. Sun, S. S. Lim, Y. M. Lam, M. Grätzel, S. Mhaisalkar and T. C. Sum, *Science*, 2013, **342**, 344.
- 13 J. H. Noh, S. H. Im, J. H. Heo, T. N. Mandal and S. I. Seok, *Nano Lett.*, 2013, **13**, 1764.
- 14 M. R. Filip, G. E. Eperon, H. J. Snaith and F. Giustino, *Nat. Commun.*, 2014, **5**, 5757.
- 15 V. D'Innocenzo, A. R. Srimath Kandada, M. De Bastiani, M. Gandini and A. T. Petrozza, *J. Am. Chem. Soc.*, 2014, **136**, 17730.
- 16 S. D. Stranks, G. E. Eperon, G. Grancini, C. Menelaou, M. J. Alcocer, T. Leijtens, L. M. Herz, A. Petrozza and H. J. Snaith, *Science*, 2013, **342**, 341.
- 17 A. Mei, X. Li, L. Liu, Z. Ku, T. Liu, Y. Rong, M. Xu, M. Hu, J. Chen and Y. Yang, *Science*, 2014, **345**, 295.
- 18 D. Liu, J. Yang and T. L. Kelly, *J. Am. Chem. Soc.*, 2014, **136**, 17116.
- 19 W. Nie, H. Tsai, R. Asadpour, J.-C. Blancon, A. J. Neukirch, G. Gupta, J. J. Crochet, M. Chhowalla, S. Tretiak and M. A. Alam, *Science*, 2015, **347**, 522.
- 20 L. Dou, Y. M. Yang, J. You, Z. Hong, W.-H. Chang, G. Li and Y. Yang, *Nat. Commun.*, 2014, **5**, 5404.
- 21 M. E. Weeks, *J. Chem. Educ.*, 1945; B. Curtouis, *Ann. Chim.*, 1813, **91**, 304.
- 22 V. P. S. Perera and K. Tennakone, *Sol. Energy Mater. Sol. Cells*, 2003, **79**, 249.
- 23 T. S. Moss, *Photoconductivity in the Elements*, Butterworths Scientific Publications, London, 1952.
- 24 A. Many, M. Simhony, S. Z. Weisz and J. Levinson, *J. Phys. Chem. Solids*, 1961, **22**, 285.
- 25 M. Hesse, H. Meier and B. Zeeh, *Spektroskopische Methoden in der organischen Chemie*, Stuttgart Georg Thieme Verlag, 2012.
- 26 J. W. Akitt, *J. Mol. Struct.*, 1985, **128**, 366.
- 27 J. J. Novoa, F. Mota, M. H. Whangbo and J. M. Williams, *Inorg. Chem.*, 1991, **30**, 54.
- 28 (a) Y. Li, F. Della Valle, M. Simonnet, I. Yamada and J.-J. Delaunay, *Nanotechnology*, 2009, **20**, 045501; (b) H. P. Zhou, Q. Chen, G. Li, S. Luo, T.-B. Song, H. S. Duan, Z. R. Hong, J. B. You, Y. S. Liu and Y. Yang, *Science*, 2014, **345**, 542.
- 29 H. W. Lin, S. Y. Ku, H. C. Su, C. W. Huang, Y. T. Lin, K. T. Wong and C. C. Wu, *Adv. Mater.*, 2005, **17**, 2489.
- 30 P. H. Svensson and L. Kloo, *Chem. Rev.*, 2003, **103**, 1649.
- 31 (a) G. Bowmaker and S. Hannan, *Aust. J. Chem.*, 1971, **24**, 2237; (b) W. Gabes and H. Gerding, *J. Mol. Struct.*, 1972, **14**, 267.
- 32 P. Deplano, F. A. Devillanova, J. R. Ferraro, M. L. Mercuri, V. Lippolis and E. F. Trogu, *Appl. Spectrosc.*, 1994, **48**, 1236.
- 33 P. D. Boyle, J. Christie, T. Dyer, S. M. Godfrey, I. R. Howson, C. McArthur, B. Omar, R. G. Pritchard and G. R. Williams, *J. Chem. Soc., Dalton Trans.*, 2000, 3106.
- 34 M. A. Petit and A. S. Soum, *J. Polym. Sci.*, 1987, **25**, 423.